SUPPLEMENTARY DATA

Methods of the supplementary data

"Coarse-to-fine subpixel" algorithm

Because pixel-level coarse coronary segmentation was insufficient for surface model reconstruction, a new "coarse-to-fine subpixel" algorithm for lumen contour was proposed to achieve more precise reconstructions (figure 1 of the supplementary data). Specifically, we first extracted the cross-sectional image along the centerline and computed its gradient map. Next, we transferred the gradient image's coordinate system to polar coordinate system. K rays shot out from the center point at fixed angles, and each ray has fixed sample points with length L. We queued the lines and obtained a 2-dimensional (D) polar image with size K* L. In this image, we computed the K highest gradient magnitude points in all lines and fitted a smooth curve. The points on the smooth curve were related to the lumen contour points.

To obtain the stable and smooth lumen boundary, we mimicked the manner of radiologists, which referred the nearest continuous multiple frames. Therefore, we extracted N nearest cross-sectional images to refine the N/2 frame lumen contour. After transferring each frame to polar coordinate system, the previous method was used to fit the curves of the highest gradient. Next, we collected all points of the fitted curves to fit the surface by the moving least squares method. Then, we extracted the curve of the N/2 frame in the fitted surface to the final curve, and each point in this curve was related to the lumen contour point in a specific angle. Finally, we mapped these points back to the Cartesian coordinate system and fitted a closed boundary by the Spline interpolation method. We used this closed contour as the final lumen boundary. To be clear, the ray number K is 32, the fixed sample point length L is 128, and the nearest cross-sectional image number N is 16.

To reconstruct the coronary tree model, precise lumen contours were generated at specified points along the coronary centerline. Typically, we extracted 1 lumen contour in each 7 centerline points. To avoid an abnormal surface shape in the coronary bend, we also generated lumen contours less than 7 points where the curvature of centerline curve was highest in the local region.

Validation by the model reconstructed from invasive coronary angiography (ICA)

To validate the "coarse-to-fine subpixel" algorithm, we compared the model reconstructed from

coronary computed tomography angiography (CCTA) images by using the “coarse-to-fine subpixel” algorithm and the model reconstructed from invasive coronary angiography (ICA) images by using 3D quantitative coronary angiography frames of different angles. Since ICA images have a higher resolution, this comparison shows us the information if the model reconstructed from CCTA is statistically larger or smaller. In total, 200 diameters were compared. The frequency of ratios is shown in figure 2 of the supplementary data. Most ratios fell in range 92% to 103%. The mean value (± SD) of the ratios was 0.99 ± 0.13. This demonstrates that the model reconstructed by the “coarse-to-fine subpixel” algorithm has a good agreement with the model reconstructed from ICA images.

Comparison of reconstruction segmentation methods of different CT-FFR techniques (table 1 of the supplementary data)

Toshiba CT-FFR and Siemens cFFR used 1D image segmentation methods for reduced-order fluid model calculation. HeartFlow FFR_{CT} adopted 3-dimensional image segmentation by using classic pixel-level segmentation. United-Imaging uCT-FFR used a machine learning algorithm to conduct 3D image segmentation. Our coarse-to-fine subpixel segmentation method results in a quite different model with pixel-level segmentation, by which the model surface reconstructed is rough (figure 3 of the supplementary).

Comparison of machines used in each medical center (table2 of the supplementary data)

This was a multicenter, prospective cohort study, which was conducted at 6 tertiary hospitals in China. Table 2 outlines the parameters of the machines used in each medical center. The "coarse-to-fine subpixel" algorithm has been demonstrated to be compatible with these diverse machines.

Table 1 of the supplementary data

Comparison of reconstruction segmentation methods of different CT-FFR techniques.

	FFR_{CT} [1]	CT-FFR[2]	cFFR[3]	uCT-FFR[4]	RuiXin-FFR
Manufacturer	HeartFlow	Toshiba	Siemens	United-Imaging	Raysight
Reconstruction model dimension	3D	1D	1D	3D	3D
Reconstruction segmentation method	Classic image processing algorithms to segment the 3D coronary artery tree, such as image segmentation, morphology	Use classic image processing algorithms to segment 4 one-dimensional images of 70%, 80%, 90%, 99% of R-R interval	1D image segmentation of coronary artery using machine learning algorithm	3D image segmentation of coronary artery tree using machine learning algorithm	3D image segmentation of coronary artery tree, then using "Coarse-to-Fine Subpixel" algorithm to achieve more precise reconstructions

CT, computed tomography; FFR, fractional flow reserve.

Table 2 of the supplementary data

Parameters of the machines used in each medical center

Medical Center	Beijing Anzhen Hospital, Capital Medical University, Beijing		Beijing Hospital, Beijing,	Sixth Medical Center of PLA General Hospital, Beijing	Liaoning Provincial People's Hospital, Shenyang	Wuhan University Renmin Hospital, Wuhan, Hubei	Zhongshan Hospital, Fudan University, Shanghai		
Machine	TOSHIBA Aquilion ONE 320	SIEMENS SOMATOM Definition Flash	SIEMENS SOMATOM Definition Flash	Philips iCT 256	SIEMENS SOMATOM Definition Flash	GE MEDICAL SYSTEMS Revolution CT	UIH uCT 960	TOSHIBA Aquilion ONE 320	SIEMENS SOMATOM Force
Thickness, mm	0.5	0.6	0.75	0.625	0.75	0.625	0.8	0.5	0.75
Pitch	0.2 ~ 0.35								
Detector number	160	128	128	128	128	256	320	160	192
Tube rotation times, sec	0.35	0.28	0.28	0.27	0.28	0.28	0.25	0.35	0.25

Figure 1 of the supplementary data

Coarse-to-fine subpixel" algorithm

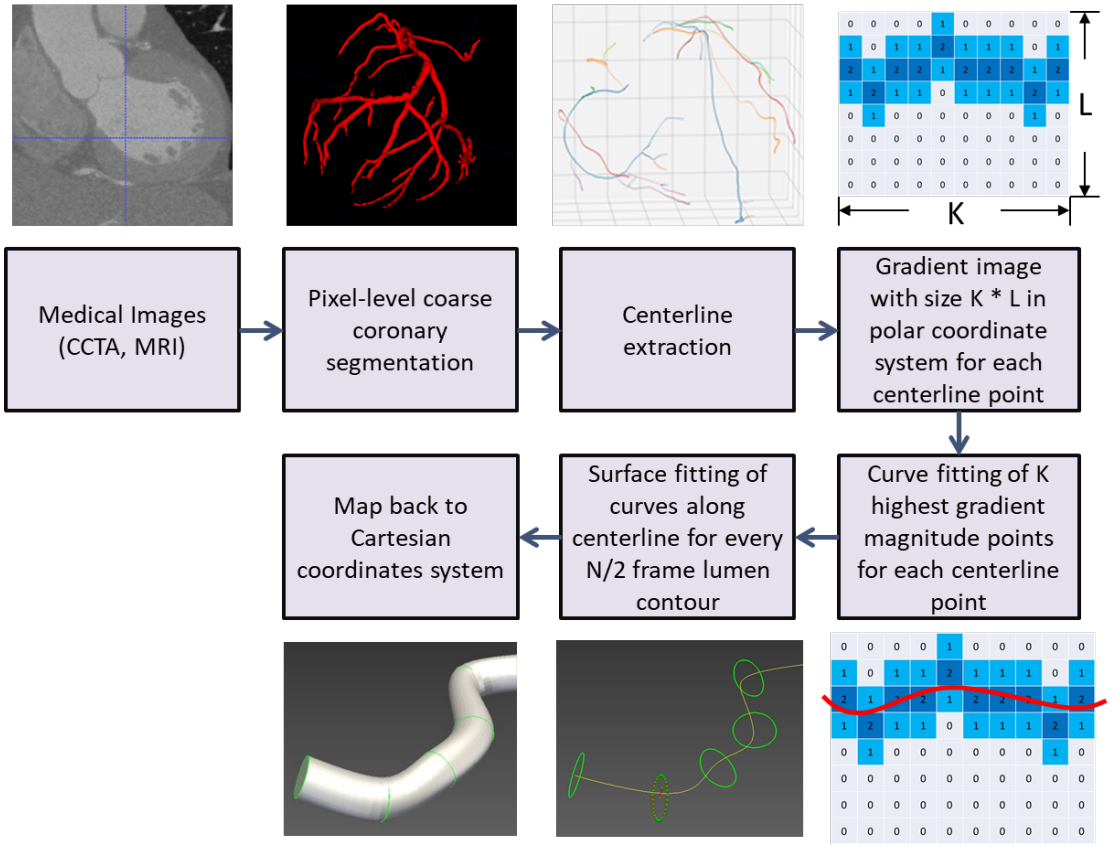

Figure 2 of the supplementary data.

Frequency of ratios of diameters reconstructed from CTA images by using the "coarse-to-fine subpixel" algorithm and diameters reconstructed from ICA images.

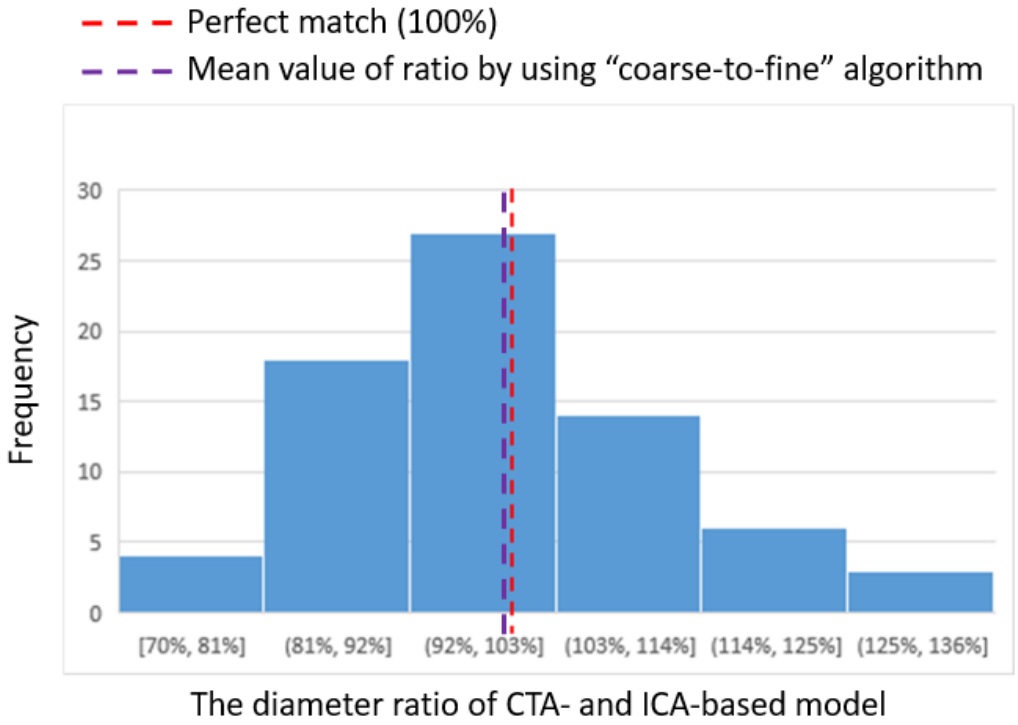

Red dashed line indicates ratio = 100%, ie, perfect match. Purple dashed line indicates the mean ratio by using the "coarse-to-fine subpixel" algorithm.

Figure 3 of the supplementary data

Comparison of models reconstructed by using pixel-level segmentation (A and C) and "coarse-to-fine subpixel" segmentation (B and D)

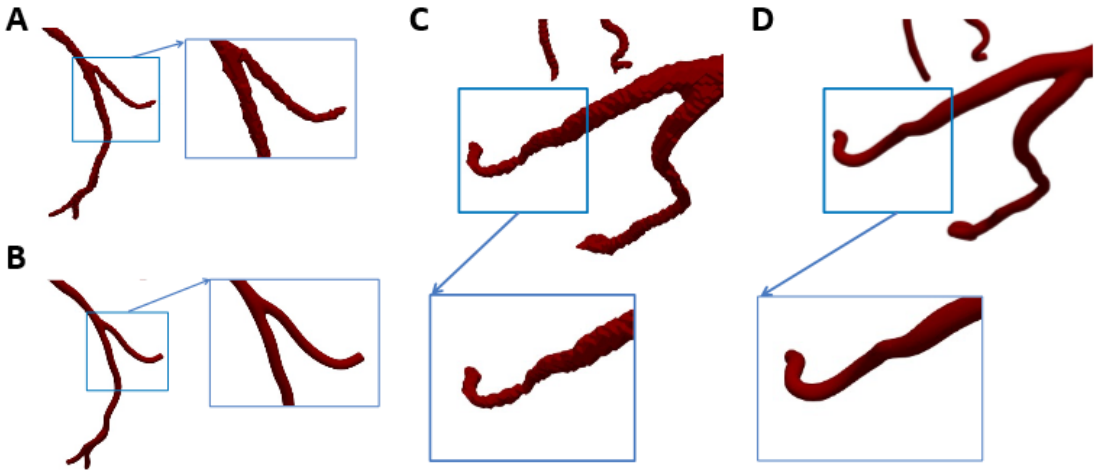

(A) and (B) are zoomed views of a vessel bifurcation. (C) and (D) are zoomed views of a vessel terminal. Compared with the coarse-to-fine subpixel segmentation method, the model surface reconstructed by using pixel-level segmentation is rough.

Figure 4 of the supplementary data

Study flowchart.

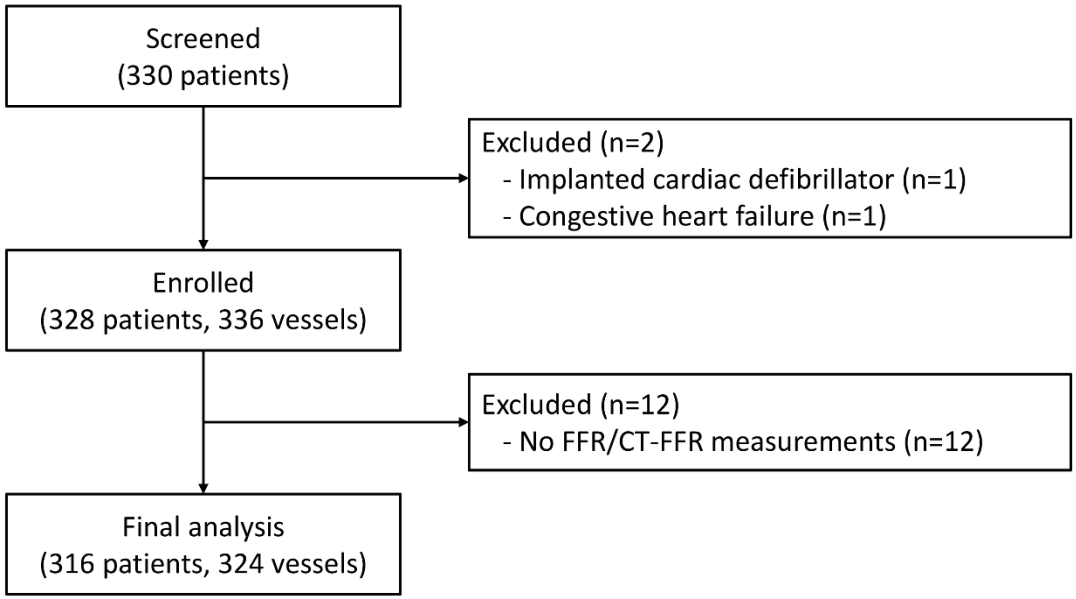

Figure 5 of the supplementary data

Diagnostic performance of CT-FFR among different FFR subgroups.

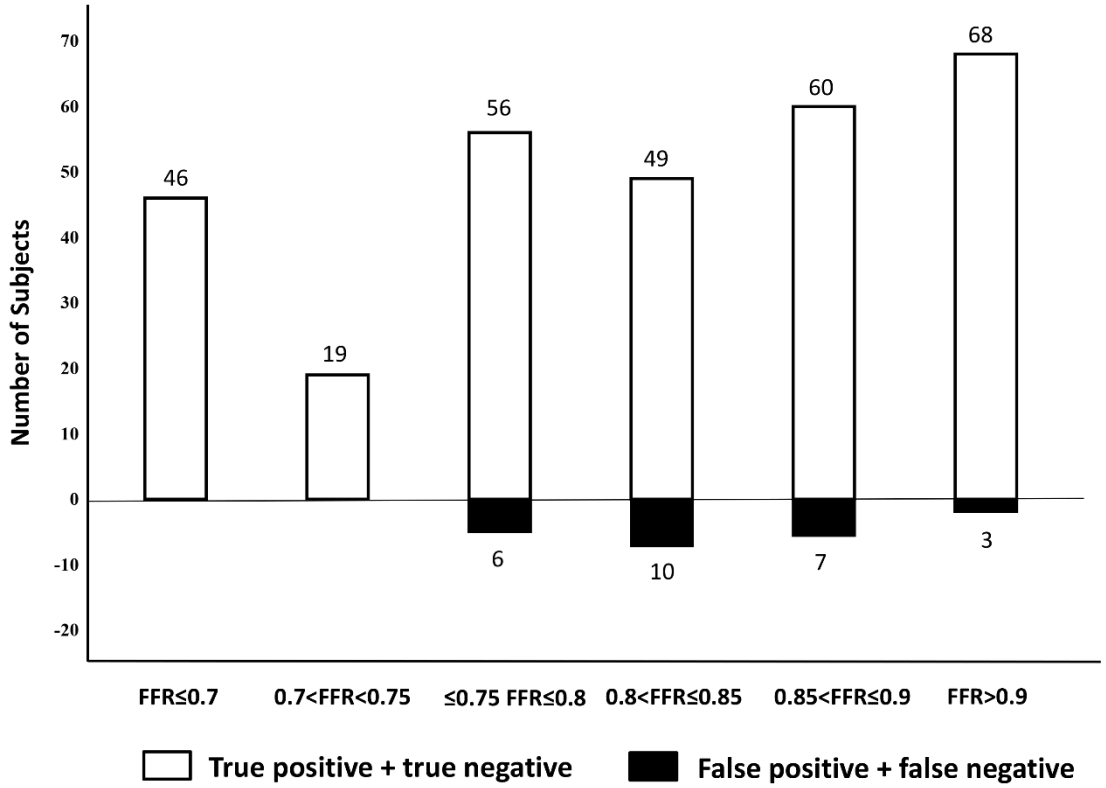

The diagnostic accuracy of CT-FFR in (true positive and true negative) discriminating hemodynamically significant stenosis among different invasive FFR subgroups. All 6 “false negative” vessels, where CT-FFR did not identify ischemia, had invasive FFR values between 0.75 and 0.80.

CT-FFR, computed tomography angiography-derived fractional flow ratio; FFR, fractional flow reserve.

Figure 6 of the supplementary data

Anatomically calcified stenosis with hemodynamically significant ischemia.

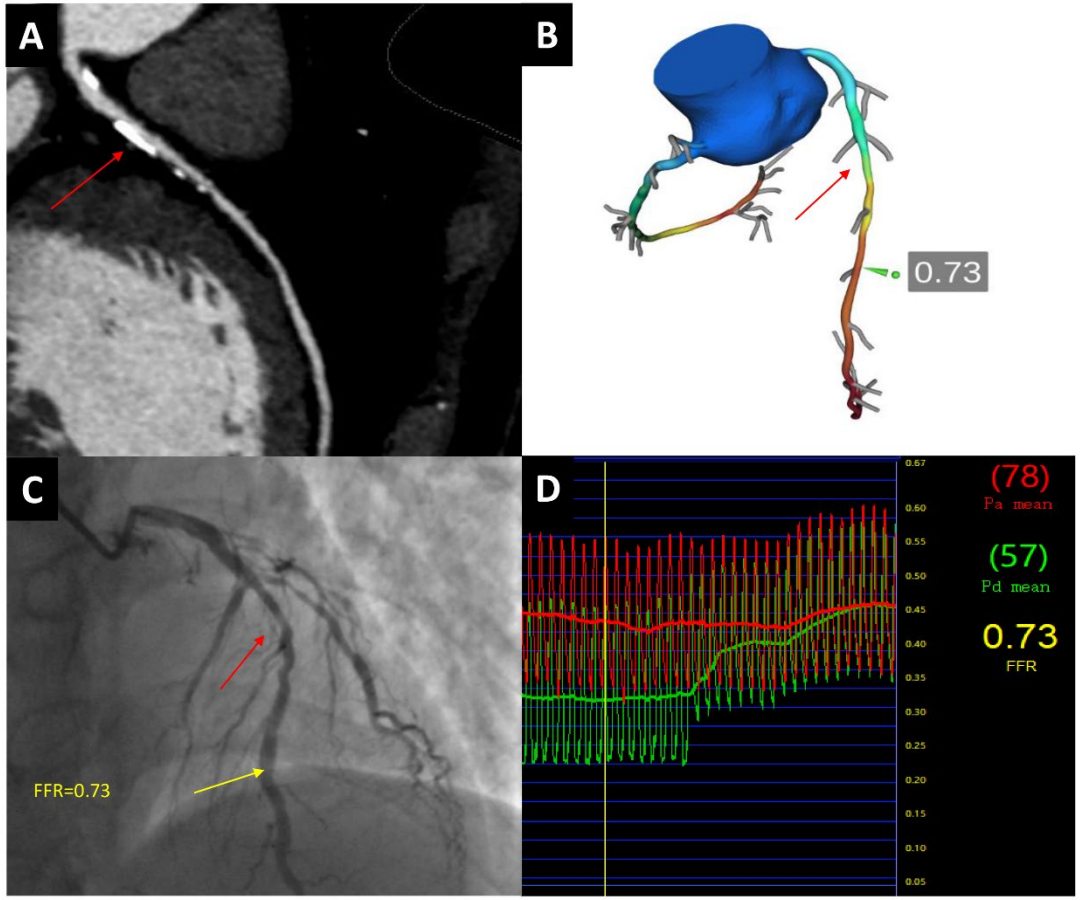

(A) CCTA demonstrating a severely calcified obstructive (70%) stenosis (red arrow) in the middle of the LAD. (B) CT-FFR demonstrates lesion-specific ischemia (0.73) (red arrow). (C, D) Invasive coronary angiography and invasive FFR confirm the obstructive lesion with FFR value=0.73 (red arrow).

CCTA, computed tomography angiography; CT-FFR, computed tomography angiography-derived fractional flow ratio; FFR, fractional flow reserve; LAD, left anterior descending.

References

1. Kim HJ, Vignon-Clementel IE, Coogan JS, Figueroa CA, Jansen KE, Taylor CA. Patient-specific modeling of blood flow and pressure in human coronary arteries. *Ann Biomed Eng.* 2010;38:3195-3209.
2. Ko BS, Cameron JD, Munnur RK, et al. Noninvasive CT-Derived FFR Based on Structural and Fluid Analysis: A Comparison With Invasive FFR for Detection of Functionally Significant Stenosis. *JACC Cardiovasc Imaging.* 2017;10:663-673.
3. Itu L, Rapaka S, Passerini T, et al. A machine-learning approach for computation of fractional flow reserve from coronary computed tomography. *J Appl Physiol (1985).* 2016;121:42-52.
4. Tang CX, Liu CY, Lu MJ, et al. CT FFR for Ischemia-Specific CAD With a New Computational Fluid Dynamics Algorithm: A Chinese Multicenter Study. *JACC Cardiovasc Imaging.* 2020;13:980-990.